Importance and effect of co-registration quality in an example of " pixel to pixel " fusion process

Philippe Blanc, Lucien Wald, Thierry Ranchin

IMPORTANCE AND EFFECT OF CO-REGISTRATION QUALITY IN AN EXAMPLE OF « PIXEL TO PIXEL » FUSION PROCESS.

(1,2) Philippe Blanc, (1) Lucien Wald, (1) Thierry Ranchin.

(1) Ecole des Mines de Paris, Groupe Télédétection & Modélisation, B.P. 207, F-06904 Sophia Antipolis Cedex.

(2) Aerospatiale, Service applications des systèmes d'observation, SE/TNE, B.P. 99, F-06322 Cannes la Bocca Cedex.

ABSTRACT:

By definition, as they require the images to merge to be superimposable, « pixel to pixel » fusion processes raise up the issue of the outcome of geometric co-registration quality on the resulting images. Indeed, local errors of geometric co-registration may introduce local errors in the merging process. Hence, we can wonder how can we define and reach the co-registration quality level that is required to minimise errors in « pixel to pixel » merging processes. The aim of this work is to understand, thanks to an example of such fusion process applied to images with different degrees of geometric distortions, the outcome of co-registration error on the fusion quality and, therefore, to measure the efficiency of some co-registration methods for the pre-processing of « pixel to pixel » merging application.

1. INTRODUCTION

The paper deals with the issue of co-registration errors between the images to merge within a « pixel to pixel » fusion process. In other words, the aim of this work is, on the one hand, to underline and to quantify the outcome of relatively small geometric distortions on the fusion quality and, in on the other hand, to define (and reach) a co-registration quality level required for « pixel to pixel » fusion process.

We have based our study on a particular fusion process: the ARSIS method. Indeed, this method is a « pixel to pixel » fusion process that is meant to increase the spatial resolution of an image (e.g. SPOT multispectral image XS) without any modification of its spectral contents by merging structures extracted from a higher resolution image of the same scene but in a different spectral band (e.g. SPOT Panchromatic image P). For more information about ARSIS, see Mangolini *et al.* (1992) and (1993).

It is important to note that the quality of such synthetic enhanced multispectral images can be efficiently assessed by the mean of the approach described in Wald *et al.* (1997) and in Mangolini *et al.* (1995). This approach has been adopted here. More precisely, SPOT XS images are down-sampled to 40 m and then synthesised by the mean of the ARSIS method at 20 m. The synthesised image XS^* are finally compared to the original image XS. In this paper, we deal with a SPOT image of the city of Barcelona, Spain. Multispectral (XS: resolution 20 m) and Panchromatic (P: resolution 10 m) images are available. The P image was acquired with an angle of 15° along the track, while the XS image was acquired at the nadir of the satellite (see Anonymous 1986). The P image has been geometrically corrected by the CNES to be superimposable to the XS one.

A technique of sub-pixel correlation has been performed onto the XS image and the P image degraded at 20 m (P_{20}): for each pixel of XS1, the best correlation with P_{20} pixels is looked for at sub-pixel level. Hence, this method provides a sub-pixel geometric deviation between each XS1 pixel with the corresponding P_{20} pixel. After filtering in order to remove the bad correlation matches, a realistic and complex field of local geometric distortions was obtained. Table 1 displays the mean and the standard deviation of those residual distortions in row and column directions. These values are relatively small but it should be noted that the field of distortions exhibits structures which are correlated to the orographic features of the scene.

	Δx	Δy
Mean	-0.27	0.28
Standard Deviation	0.08	0.11

Table 1. Means, standard deviations in pixel of the geometric distortion field in column and line direction (respectively Δx and Δy).

Here, for our demonstration, we have used mostly XS1 and XS2 image. The P image was only used to produce a field of typical and realistic local distortions. In the following, XS1 is assumed to be the image with the highest resolution (20 m) while XS2 has been down-sampled to 40 m to be the lowest resolution image noted $XS2_{40}$.
More precisely, the study is carried out in two phases. The first one is meant to underline the influence of small geometric distortions between the images to merge with the ARSIS method. The second phase consists in the assessment of the benefits of a particular co-registration method as a pre-processing of the fusion.

2. INFLUENCE OF LOCAL GEOMETRIC DISTORTIONS.

The ARSIS method was performed on the XS1 image (resolution 20 m) and the down-sampled $XS2_{40}$ image. It provided a synthesised image $M1\_XS2^*$ (resolution 20 m) which was compared, visually and quantitatively, to the original XS2 image.
Figure 2 shows the original XS2 image (a) and the synthesised $M1\_XS2^*$ image (b). One can note that there is no visual differences between the two images. Moreover, in the lines M1 of Tables 2 and 3 are reported statistical criteria which quantify the differences between XS2 and $M1\_XS2^*$ following the work of Wald *et al.* (1997). Those values are very near to the ideal values, thus confirming the visual inspection and supporting the ARSIS method as an efficient one. This comparison between XS2 and M1_XS2* is meant to be a reference for the following demonstration.
To measure the influence of the local geometric distortions, the XS1 image was re-sampled into a new image S_XS1 image by injecting the realistic field of residual geometric distortions discussed in introduction. It means that S_XS1 and XS2 are close to be superimposable but small, realistic and spatially variable geometric distortions exist and are perfectly known at each point. The ARSIS method was then performed on S_XS1 and $XS2_{40}$ images to produce a second synthetic image $M2\_XS2^*$ to be compared to $M1\_XS2^*$. This first phase of the study is illustrated in Figure 1.

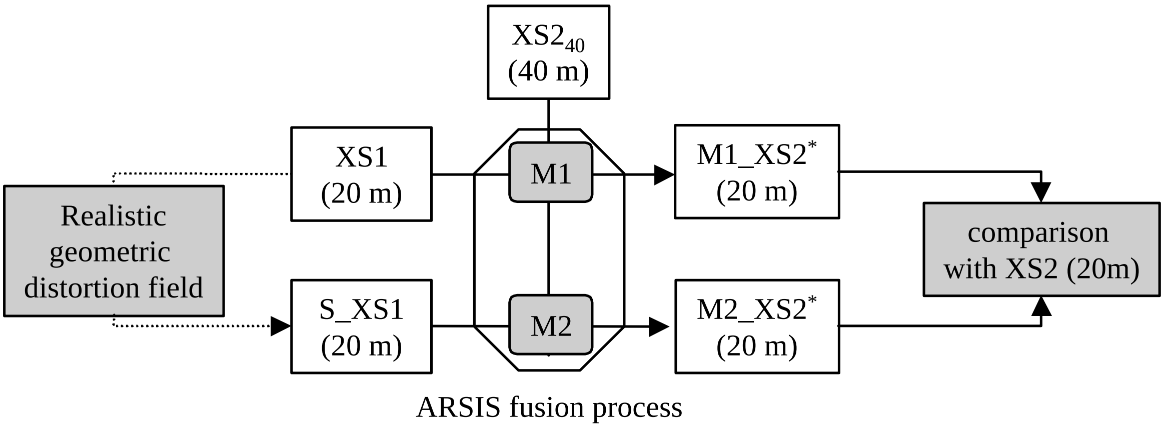

Figure 1. Illustration of the assessment of the influence of geometric distortion errors in the ARSIS method.

The quality of the M2_XS2* image can be firstly analysed and compared to XS2 and M1_XS2* by a visual inspection (see Figure 2 c). This image clearly presents artefacts near discontinuities and structures that degrades the quality of the synthesised image. In other words, on account of the local geometric distortions, the ARSIS method injects into $XS2_{40}$ non-relevant high resolution structures from S_XS1 image because they are slightly shifted. The statistic criteria given in the lines M2 of the Tables 2 and 3 corroborate the visual inspection: according to the correlation coefficient, the standard deviation of the difference and the relative error probability, the small geometric distortion field degrades notably the quality of the results of the ARSIS method. Nevertheless, we have to note that the difference of variances, that is a measure, to some extent, of the quantity of information added (negative value) or lost (positive value) during the enhancement, is better for M2 than for M1. Indeed, in the M1 case, the ARSIS method slightly increases the amount of information (about 2.3 %). This increase of information is less important for M2 (about 0.4 %). This can be explained, in part, by the fact that, in this case, the ARSIS method injects high frequency structures extracted from S_XS1 that have been smoothed by the re-sampling.

(a)

(b)

(c)

Figure 2. (a) Sub-region of the original XS2 image. (b) Same but for the synthesised M1_XS2* image. (c) Same but for the synthesised M2_XS2* image.

	Bias (ideal: 0)	Variance of XS2 - var. of XS2* (ideal: 0)	Correlation coefficient (ideal: 1)	Standard deviation of the difference (ideal: 0)
M1	0.00 0.0 %	-2.3 -1 %	0.995	1.6 3 %
M2	0.00 0.0 %	-0.4 -0.2 %	0.990	2.1 4 %

Table 2. Statistical criteria (bias, difference of variances, correlation coefficient and standard deviation of the difference) in radiance ($W.m^{-2}.sr^{-1}.\mu m^{-1}$) for comparison between XS2 and XS2* for the merging processes M1 and M2.

	0.001	1	2	5	10	20
M1	30	30	55	92	100	100
M2	23	24	43	82	98	100

Table 3. Probability (in percent) for having in a pixel a relative error less than or equal to the thresholds noted in the first row for the different merging processes. The ideal value is 100 as early as the first threshold 0.001 %.

The comparisons between the lines M1 and M2 in Tables 2 and 3 demonstrate the noticeable influence of small local geometric distortions.

As a conclusion, small geometric residual distortions that are usually encountered in images made superimposable by standard methods have a noticeable influence on the quality of products resulting from fusion processes. Only the ARSIS method was applied here, but it is believed that the effects are similar for any « pixel to pixel » fusion process.

3. THE BENEFIT OF AN ANDVANCED CO-REGISTRATION METHOD

This section explores the potentialities of an advanced co-registration method to correct residual distortions and ,thus, providing better fusion products of better quality. For this work, we applied a co-registration method to the image S_XS1 to produce a re-sampled image R_XS_1 the most superimposable to XS_1 as possible. Once applied to this R_XS1 and $XS2_{40}$ images, the ARSIS method produces another synthetic image noted $M3\_XS2^*$ that will be compared to the original image XS2. This second phase of the study is illustrated in Figure 3.

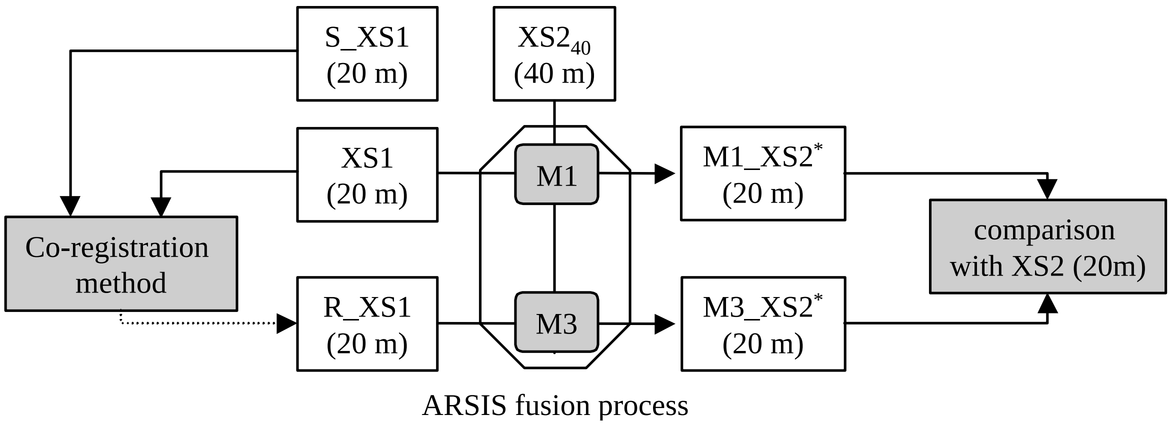

Figure 3. Illustration of the assessment of the benefit of the co-registration method as a pre-processing of the ARSIS method.

The applied co-registration method applied is a fully automatic registration method based on multiresolution analysis and local distortion model. This method is in fact an improved version of a co-registration method developed by Djamdji *et al.* (1993). The control points are detected at the lower resolution where the smoothed images present only few structures. The catching between the two sets of control points provides a first estimation of the deformation model. Then this estimation is refined as the resolution gets finer till the original resolution. Validation tests have shown that this method provides a large number of good matched control points. This enables the use of local geometric distortion models. In other words, this method is well fitted to correct small and local geometric distortions.

In our case, we perfectly know the distortions between the two images S_XS1 and XS1. Therefore, we can accurately measure the co-registration error after the geometric correction. Table 4 gives some statistical criteria to describe it and can be compared to Table 1.

	Δx	Δy
Mean (ideal: 0)	-0.03	-0.04
Standard Deviation (ideal: 0)	0.05	0.06
Correlation (ideal: 1)	0.78	0.85
Difference of variances in percent (ideal: 0)	-7.8 %	-8 %

Table 4. Means, standard deviations in pixel for the error of the co-registration method in the column and row directions (respectively Δx and Δy). Correlation and difference of variances are also reported (see text).

First, we notice that the bias and the standard deviation resulting from this co-registration Compared to the Table 1, the gain in bias is spectacular. Nevertheless, the bias and the standard deviation are not totally relevant to describe local co-registration errors. Two other statistic criteria are then used:

- *the difference of variances:* this value is, to some extend, the difference of the quantity of information between the actual distortions and the estimated ones.
- *The correlation coefficient:* it shows the similarity in shape between the actual and the estimated distortions.

Those criteria are close to the ideal value. It means that the co-registration process has well corrected the local geometric distortions between S_XS1 and XS1.

Let examine, now, the synthetic image M3_XS2*. As far as visual analyses are concerned (Figure 4), this image does not present the same artefacts than in M2_XS2*. Moreover, except for the difference of variances (for the same reason than in M2 case), the statistic criteria given in Tables 5 and 6, show that the level of quality of the fusion is equivalent to the M1 case. In other words, the co-registration method has been almost efficient enough to correct the local geometric deviation for the fusion process.

Figure 4. As Figure 2, but for the synthetic image M3_XS2*.

	Bias (ideal: 0)	Variance of XS2 - var. of XS2* (ideal: 0)	Correlation coefficient (ideal: 1)	Standard deviation of the difference (ideal: 0)
M3	0.00 0.0 %	1.8 0.8 %	0.995	1.6 3 %

Table 5. As Table 2, but for the ARSIS merging process M3.

	0.001	1	2	5	10	20
M3	28	29	53	91	99	100

Table 6. As Table 3, but for the ARSIS merging process M3.

4. CONCLUSION

We have studied the influence of geometric distortion in a very realistic, typical and controlled case. Despite the weakness of those small geometric distortions mean and standard deviation are, in this case, respectively less than 0.3 and 0.1 pixel, it was shown that it noticeable on the quality of products resulting from a “pixel to pixel” fusion process as far as visual and quantitative assessments are concerned.
The example shown here is based on SPOT images and ARSIS fusion method. It is important to note that those conclusions can be extended to other sensors and other fusion methods such as IHS method (see Harris and Murray 1990) or the high frequency injection technique developed by Munechika *et al.* (1993).
Moreover, we have pointed out the need for a better accuracy in co-registration prior to “pixel to pixel” fusion processes. An advanced method of automatic co-registration using multiresolution analysis and local geometric distortion models has been successfully tested. It constitutes an answer to the need of high quality co-registration underlined previously.

<u>REFERENCES:</u>

Anonymous, 1986. *Guide des utilisateurs de données SPOT*, 3 volumes, Editors CNES and SPOT Image, Toulouse, France.

Djamdji, J.P., A. Bijaoui, and R. Manière, 1993. A new method of automatic registration, based on a multiresolution decomposition of the images using the wavelet transform, *Photogrammetric Engineering & Remote Sensing*, 59(5):645-653.

Harris, J.R., and R. Murray, 1990. IHS transform for the integration of radar imagery with other remotely sensed data, *Photogrammetric Engineering & Remote Sensing*, 56(12):1631-1641.

Mangolini, M., T. Ranchin, and L. Wald, 1992. *Procédé et dispositif pour augmenter la résolution spatiale d’images à partir d’autres images de meilleure résolution spatiale*, French patent n° 92-13691, 20 November 1992; *Methods and Devices for Increasing the Spatial Resolution of Images from Other Images of Better Spatial Resolution*, USA patent serial 08/249,882, 26 May 1994.

Mangolini, M., T. Ranchin, and L. Wald, 1993. Fusion d’images SPOT multispectrales (XS) et panchromatique (P), et d’images radar. *De l’optique au radar, les applications de SPOT et ERS*, Cepaduès-Editions, 111 rue Vauquelin, Toulouse, France, pp. 199-209.

Mangolini M., T. Ranchin, and L. Wald, 1995. Evaluation de la qualité des images multispectrales à haute résolution spatiale dérivées de SPOT, *Compte-rendus du colloque « Qualité de l’interprétation des images de télédétection pour la cartographie »*, Grignon, 1-3 September 1995, *Bulletin de la Société Française de Photogrammétrie et Télédétection*, 137:24-29.

Munechika, C.K., J.S. Warnick, C. Salvaggio, and J.R. Schott, 1993. Resolution enhancement of multispectral image data to improve classification accuracy, *Photogrammetric Engineering & Remote Sensing*, 59(1):67-72.

Wald, L., T. Ranchin, and M. Mangolini, 1997. Fusion of Satellite Images of Different Spatial Resolutions: assessing the quality of resulting images, *Photogrammetric Engineering & Remote Sensing*, 63(6):691-699.